Applied Physics A (# 4807) manuscript No.
(will be inserted by the editor)

Stable C atom displacements on HOPG surface under plasma low energy argon ion bombardment

Bernard Rousseau[1], Henriette Estrade-Szwarckopf[1], Anne-Lise Thomann[2], Pascal Brault[2,⋆]

[1] Centre de Recherche sur la Matière Divisée, UMR6619 CNRS-Université d'Orléans, 45071 Orléans Cedex 2, France

[2] Groupe de Recherches sur l'Energétique des Milieux Ionisés, UMR6606 CNRS-Université d'Orléans BP 6744, 45067 Orléans Cedex 2, France

Received: January 21,2002 / Revised version: June 10, 2002

Abstract Surface defects are generated by an Ar-plasma on crystalline graphite. *In-situ* Scanning Tunneling Microscopy reveals localized defects surrounded by $\sqrt{3}$x$\sqrt{3}$ R30° superstructure (Friedel's charge oscillations) for short treatment time samples and long range disordered lattices for longer treatment times. *In-situ* X-ray Photoelectron Spectroscopy C1s core level spectra exhibit a broadening attributed to a distribution of C atoms in inequivalent sites. As implantation of heteroatoms and formation of vacancies can be ruled out, defects are attributed to stable displaced surface carbon atoms.

PACS: 81.65.Cf, 68.35.Dv, 68.37.Ef, 79.60.Ht

Inducing defects on substrates prior to thin film deposition is an interesting way to modify the growth mode and control the deposit morphology [1]. For example, monodispersed and well-organized nanoparticles may be obtained on a properly prepared substrate. In order to understand how defects may drive thin film growth, it is necessary to precisely control their formation but also to define their nature accurately.

Many authors have reported on Highly Oriented Pyrolithic Graphite (HOPG) surfaces modified by ion beam or plasma in a large energy range from tens of eV to tens of keV [2–11]. The nature of such defects has been proposed to be : vacancies, interstitial atoms originated from the beam or plasma ions (Ar, Kr, C, O), interstitial

⋆ e-mail: Pascal.Brault@univ-orleans.fr

C atoms displaced by the ions, C clusters, C-H bonding in the case of H^+ plasma, ... In the low energy range($<$ 100 eV), different interpretations have been suggested for defects that give identical STM images. The nature of these defects thus remains unclear.

In this work, HOPG surfaces are submitted to low pressure Ar plasma and characterized in situ by X-ray Photoelectron Spectroscopy (XPS), UV-Photoelectron Spectroscopy (UPS) and Scanning Tunneling Microscopy (STM), all working in the same UHV system. Indeed, few of the above mentioned papers report analysis results of techniques coupled with STM. For instance graphite surfaces submitted to O-plasma [11] and observed by STM seem to exhibit vacancies or at least low charge density of states (CDOS) sites, attributed to oxygen bound carbons. Unfortunately the presence of surface oxygen atoms was not checked by XPS nor AES. Moreover, while most of the HOPG surfaces were treated under clean atmosphere, many of them were analyzed by STM after a transfer in air, which could be responsible for a change in their state. In the present study we show that simultaneous in-situ chemical, structural and electronic analyses are required for the unambiguous identification of surface defects.

The chosen STM and UPS techniques are obviously sensitive to the first or to the two outermost atomic layers. XPS explores more deeply, down to about 10 layers but the two external layers contribute about 50% of the signal and a careful analysis of the peak shape enables the volume states to compared with the surface states. Moreover, the interpretation of the spectra of this technique is far easier than those of AES and does not need any external assumptions. Lastly, XPS can detect almost all the chemical elements (except hydrogen) present on the surface (sensitivity limit $\approx 1\%$).

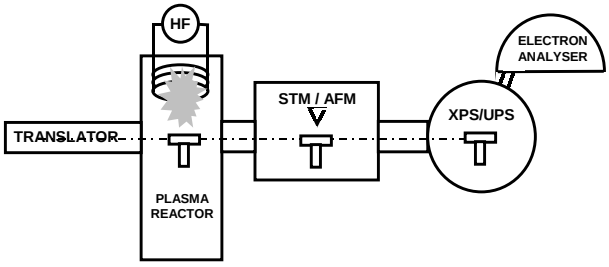

Fig. 1 Schematic of the experimental setup

1 Experiments

The experimental set up is presented in Fig. 1, it is composed of three main chambers : the plasma reactor (base pressure between treatments 10^{-7} Pa) connected to an UHV (10^{-8} Pa) apparatus composed of STM (Park Scientific) and XPS / UPS (VG ESCALAB) chambers. This configuration allows the treatment and the analysis of the surface without air exposure.

The plasma is initiated in argon gas at a fixed 10 Pa pressure via a stainless-steel antenna connected to an HF (100 MHz) power supply. The input power is quite low, close to 5 W and the antenna-substrate distance is about 13 cm. With an electrically floating substrate holder, the

ions present inside the plasma will be accelerated by the negative self-bias potential ≈ -20 V created between the plasma and the surface [12]. In the present configuration the ion flux reaching the substrate surface is of the order of 10^{13} cm^{-2} s^{-1}. These experimental conditions are kept constant except the treatment time which is varied from 1 min to 30 min, in order to, first, create isolated defects, and then, to induce more extended perturbations.

STM imaging is performed at room temperature in constant current mode (0.3 - 0.5 nA) with an applied bias of 30 mV. The images are recorded with scan rates of 0.5 to 20 Hz depending on the scale. The tips are Pt-Ir wires cut with a grip. The photoelectron spectrometer is equipped with a Mg Kα (hν = 1253.6 eV) anode and a helium discharge lamp (hν = 21.2 eV) for XPS and UPS analysis respectively. The resolution of the instrument at 20 eV pass energy is about 0.2 eV. The spectrometer calibration is performed on a gold sample (Au4f peak at 84.0 eV).

Very high quality graphite samples (HOPG provided by Dr. A. Moore, Advanced Ceramics, USA) are introduced in the UHV chamber and in situ cleaved perpendicular to the c axis. During this latter procedure the substrate holder is cooled with liquid nitrogen. Surface cleanliness is checked by XPS as well as by UPS before transfer to the STM chamber. The graphite lattice is controlled both at atomic level and large scale by STM measurements on the original surfaces. After plasma treatment, the HOPG is analyzed successively by UPS, XPS and finally by STM. Several samples have also been removed from the UHV chamber and observed by STM in air, in order to check the treated surface stability after air exposure.

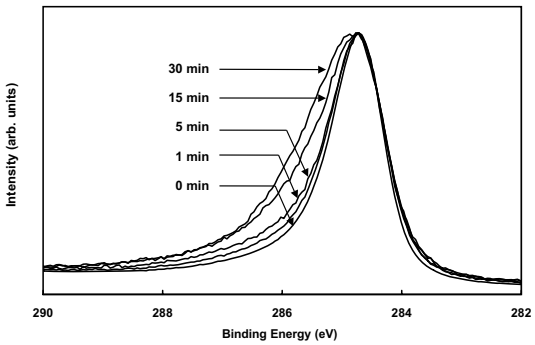

Fig. 2 XPS spectra taken at successive exposure times showing the progressive broadening of the C1s core level line.

2 Results and discussion

One of the main characteristics of the defects observed in the present work is their temporal stability. Several months after the surface preparation, the recorded XPS spectra are identical to those obtained immediately after defect creation, when the surface is kept under UHV. Similarly, the STM recorded images are equally stable, whatever the atmosphere in which the surface is kept, air or UHV.

XPS C1s spectra of HOPG surfaces before and after plasma treatment are shown in Fig. 2. The unmodified HOPG spectrum is composed of two well known struc-

tures : the main asymmetrical peak at 284.5 eV with a 0.9 eV FWHM (as measured in our apparatus), and a broad energy loss peak shifted by about + 6 eV attributed to $\pi - \pi^*$ transitions (plasmon). The C1s spectrum exhibits the same shape in natural graphite, pyrographites and in partly graphitized pyrocarbons, composed of relatively extended almost parallel graphene layers not yet 3D structured. The common characteristics of all these carbon types are the flat sp^2 type character of the carbon layers which leads to the specific C1s spectrum described here.

It can be seen on Fig. 2 that, when the treatment time is increased, the C1s peak of the Ar plasma HOPG treated surface broadens on the high energy side. There is no unique solution for fitting such a spectrum and for its interpretation, two main points should be kept in mind: 1) the low energy Ar^+ ions are not able to perturb the HOPG surface deeper than the first two planes [13,14]; 2) XPS technique allows to analyze about ten atomic layers but the contribution to the total signal of the two outermost ones is at least 50 % at normal emission. Thus, the XPS C1s spectra will be composed of two contributions : one arising from the unperturbed underlying graphite layers (all parameters being fixed by fitting the spectrum of the pristine untreated HOPG) and one from the two upper layers modified by the plasma treatment. Fitting the complete spectrum results in the sole determination of the unknown parameters of the perturbed surface. We found that this new contribution could be fitted with a unique peak, $\approx +0.8$ eV high energy shifted. Its parameters are kept constant, (symmetrical, FWHM $\approx$ 2.2 eV), independent of the treatment time except its intensity which increases with the exposure time. This new peak is already noticeable for a treatment time as short as 1 minute and concerns 1 - 2 % of the total observed carbon population (2-4 % of the outermost C atoms) while it reaches 30% after 15 minutes treatment. This peak has undoubtedly to be related to the perturbed surface carbon atoms and thus to the created defects. Its large FWHM (2.2 eV) means that the corresponding perturbated surface is composed of a distribution of unequivalent carbon sites. In the following, it will be called the "C1s defect peak" and its relative population (multiplied by 2 in order to have the corresponding population of the outermost layers) is given in Table 1. An example of a C1s spectrum decomposition is given Fig. 3 for the 30 min treatment sample on which the C1s defect peak contributes about 45% of the total observed carbon population, i.e. $\approx$ 90-100% of the outermost layers. A peak corresponding to the C-O or C-OH bonds has also been added (at about +2 eV) taking account of the O/C ratio ($\approx$3%) determined from both C1s and O1s spectra. Its minute intensity does not depend on the treatment duration and thus is not related to the defects.

On this long time treated surface, except for some % of oxygen mentioned above, we do not detect by XPS any trace of heteroatoms, neither metal which could be

Table 1 Characteristics of the damaged surfaces (See text).

treatment time	C population in C1s defect peak	mean diameter	mean height	fraction of perturbed area
(min)	(%)	(nm)	(nm)	(%)
1	2-4	1.4	0.5	3-6
5	30	2.0	0.9	-
15	60	4.6	1.3	-
30	90-100	5.5	1.1	100

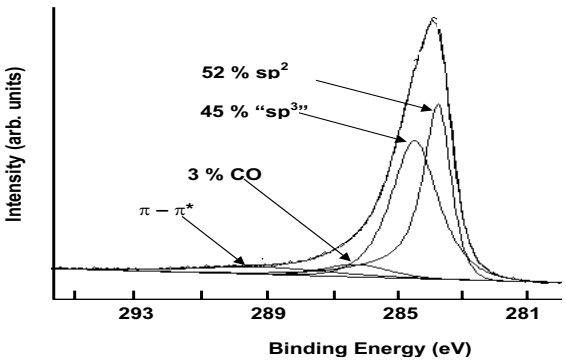

Fig. 3 Decomposition of the XPS C1s core level line taken at t=30 min exposure time.

sputtered by the plasma ions from the different devices inside the plasma reactor, nor argon which could be implanted between the first atomic planes.

Hydrogen is not detectable by XPS but may play a role in the surface perturbation and this role is worth discussing in greater details. Indeed, a recently published paper has been devoted to defects created on an HOPG surface by a hydrogen plasma [10]. For treatment conditions close to ours, their results are quite similar as far as STM images (defect appearance and density) for short treatment times and UPS and XPS spectra for long duration are concerned. As in our study, the authors fit their XPS spectrum by assuming a new 1 eV high energy shifted peak. The created defects are claimed to be C-H bonds, known to give rise to a 0.4-0.5 eV high energy shifted C1s peak.

Because of the surprising likeness between their results and ours, we looked for the presence of hydrogen in our experiment and tried to defined its eventual role. In all UHV chambers, the hydrogen originates in the dissociation of water and because of that common origin, the hydrogen concentration is always of the same order of magnitude as that of oxygen. When the plasma is switched on, water is rapidly desorbed from the chamber walls producing a temporary increase of hydrogen and of oxygenated species partial pressures. This increase leads to the formation of oxygen carbon bonds detected by

XPS on the sample surface. After 1 minute of plasma treatment, the corresponding relative population is 2-3%, and remains constant whatever the treatment time. As measured by mass spectrometry (plasma off), the residual hydrogen partial pressure is 10^8 times smaller than that of argon in our plasma or of hydrogen in the case of Ref. [10] (10 Pa gas pressure). Such a low concentration cannot be responsible for the creation, during the same treatment duration, of same number of defects as the H^+ are, in a pure hydrogen plasma. Thus the defect creation must be due to the ions (Ar^+ or H^+) present in both types of plasma, irrespective of their chemical reactivity. Even if hydrogen is not responsible for the defect creation in our case, it may play a role in an eventual stabilizing process. Indeed, it might be thought that the created defects consist of highly unstable structures such as dangling bonds. Dissociated hydrogen could be fixed on these bonds but it is even scarcer than molecular hydrogen (dissociation probability around 10^{-7} in our plasma), too scarce to stabilize all the created defects. Molecular hydrogen has a chance to react with "dangling bonds", but since the formation enthalpy of C-H bonds is slightly lower than the H-H one, this process seems very unlikely in our conditions. In the hypothesis that defects are unstable dangling bonds, they would interact with oxygen as well as with hydrogen which are in same minute concentrations in our chamber. However, the XPS detected C-O bonds number does not increase with treatment duration as does the total defect number.

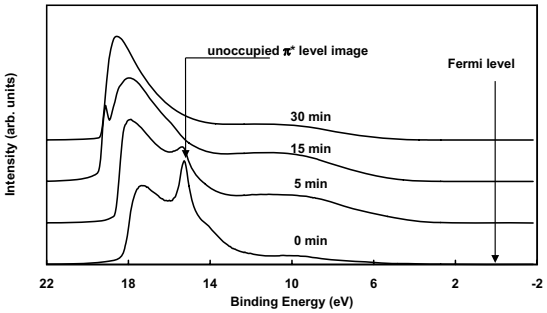

Fig. 4 UPS spectra taken at successive exposure times t showing the extinction of the π^* level image peak when increasing time.

Thus, we have to conclude that the defects are not unstable and reactive and hence, we rule out the existence of dangling bonds stabilized as C-H or as C-O bonds. We have to look for another type of defects.

UPS spectra of the 5, 15 and 30 minutes samples, together with the pristine HOPG surface one are presented in Fig. 4. It can be seen that the unoccupied π^* level image peak (at apparent energy $E_b \approx 15$ eV), characteristic of a clean graphite surface [15], progressively vanishes without any energy shift as the plasma treatment time increases. This indicates a loss of the carbon π functions in the outermost graphene planes. The abrupt decrease in the intensity visible around 20 eV binding energy, due to the UV lamp cut off, is continuously shifted towards higher binding energies, denoting a work function decrease with increasing exposure time, also related with the damages created on the surface.

We therefore investigated whether our STM results are compatible with such a conclusion of modifications of the outermost planes. STM images obtained for 1 min and 30 min exposure time samples are given in Fig. 5a, 5b (50 nm x 50 nm); 5c, 5d (20 nm x 20 nm) and 5e, 5f (5 nm x 5 nm). Defects appear as hillocks with density and size increasing with treatment duration. Their mean diameters increase from about 1.5 to 5.5 nm and their apparent height from 0.5 to 1 nm. These values are given in Table 1.

After a short time plasma exposure, the defects clearly appear well localized (fig. 5a, 5c, 5e). Like many previous authors, we tried to observe those isolated defects by other near field microscopy such as contact-AFM, but unsuccessfully, probably because of lack of sensitivity (about 0.1 to 0.2 nm in the event of corrugation) and/or lack of lateral resolution ($\phi < 10$ nm) due to the tip dimensions.

Such defects inducing an increase in STM signal, could be interpreted as vacancies. Indeed, DOS calculations reported by Hahn et al. [6,9] predict an increase of the charge density of state near Fermi energy (CDOS) and thus of the STM signal on the atoms surrounding a vacancy. While monoatomic vacancies are stable and can appear as small protuberances in STM images, this would certainly not be the case for extended vacancies [6,9,16,17]. Indeed, one would expect to find a treatment duration (maybe not the longest one) for which holes are evidenced by STM and even by AFM, as reported for surfaces treated by an oxygen plasma [11]. On the contrary, in our case, features are always observed as protrusions, which increase both in diameter and height with treatment duration. Unfortunately, it is not possible to compare this evolution with previous work [2–11], since only isolated defects were considered, and not those originating from long treatment times.

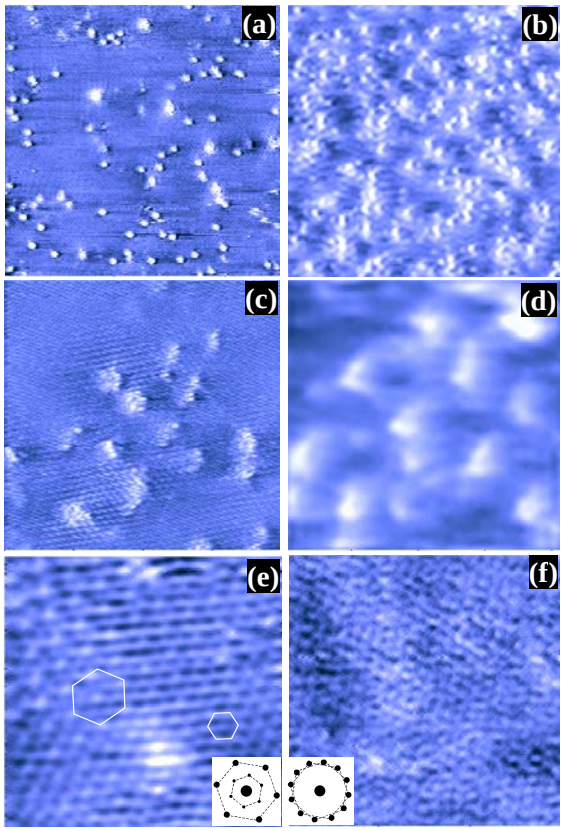

Fig. 5 STM images of the defect growth and morphologies. (a) t= 1 min, 50 nm x 50 nm,(b) t= 30 min, 50 nm x 50 nm, (c) t= 1 min, 20 nm x 20 nm,(d) t= 30 min, 20 nm x 20 nm, (e) t= 1 min, 5 nm x 5 nm, (f) t= 30 min, 5 nm x 5 nm. The insets show schematic 2D-FT of images e) and f)

A question rises at this step : do the argon ions, present in the plasma, carry enough energy to create vacan-

cies? Hahn et al. [9] report that using well defined energy Ar ion beam, isolated defects, very similar to ours, become visible by STM, only with Ar^+ energies higher than 40 eV. Moreover, calculations and experiments [5, 13] also show that for Ar^+ impinging ions, the displacement threshold of a carbon atom leaving a vacancy at the HOPG surface is about 47 eV, the penetration energy 43.5 eV and the sputtering threshold 70 eV [18]. During the low pressure plasma treatment, the substrate is mainly submitted to the effect of Ar^+ ions, but other species carrying less energy may reach the surface. Neutral and metastable (carrying an energy of about 10 eV) Ar atoms statistically also impinge onto the surface, as well as oscillating electrons (HF field) [19]. In our experiments, the maximum ion energy is relatively weak, i.e. about 20 eV. At 10 Pa pressure, due to collisions with Ar atoms on their way to the surface, only 20-40 % of the Ar^+ ions gain this maximum energy [20,21]. Following Hahn *et al* [9] such an energy would not be high enough for the Ar ions alone to create vacancies, induce implantation nor sputtering on the HOPG surface. However, our results show that some special effect of the plasma has to be considered. Even if the plasma species cited above have individually a too low energy to be efficient, they may act on the surface, hit it and make it more sensitive to ion effects. In such a case, all the thresholds may be lowered. It is already known for plasma-materials interactions that the collective effect of the plasma active species is more efficient than the sum of the individual processes[22]. Such a phenomenon, called the synergetic effect, to which metastable atoms, electrons, photons and ions contribute, is often invoked even if it is not yet clearly elucidated.

In any case, even if thresholds are expected to be lowered by the other plasma species action, the vacancy creation threshold remains higher than the penetration one and no Ar implantation has been observed. Thus, it may be concluded that neither the isolated defects nor the completely damaged surfaces result from vacancy creation, which in any case would involve the presence of dangling bonds ruled out above.

On images obtained after a short time plasma exposure, between the isolated hillocks, the usual HOPG lattice remains unperturbed (Fig. 6), as a plane hcp like structure (only one in two C atoms is detected). An isolated defect is also present on this image with its height profile. From this detailed structure, the defect appears to be composed of several carbon atoms apparently elevated above their lattice sites. Indeed, the HOPG lattice is not disturbed on the top of the defect, the regular C-C distance just being slightly larger ($a \approx 0.29$ instead of 0.25 nm). Around most defects a lattice superstructure is evidenced as a height modulation shown on Fig. 5c and 5e. The amplitude of this modulation decays from a maximum (relatively low < 0.2 nm) at the center of the defect within a distance of about 4 nm along the graphite lattice. Such a superstructure is clearly visible on Fig. 5e, where large size hexagons composed of elevated carbon

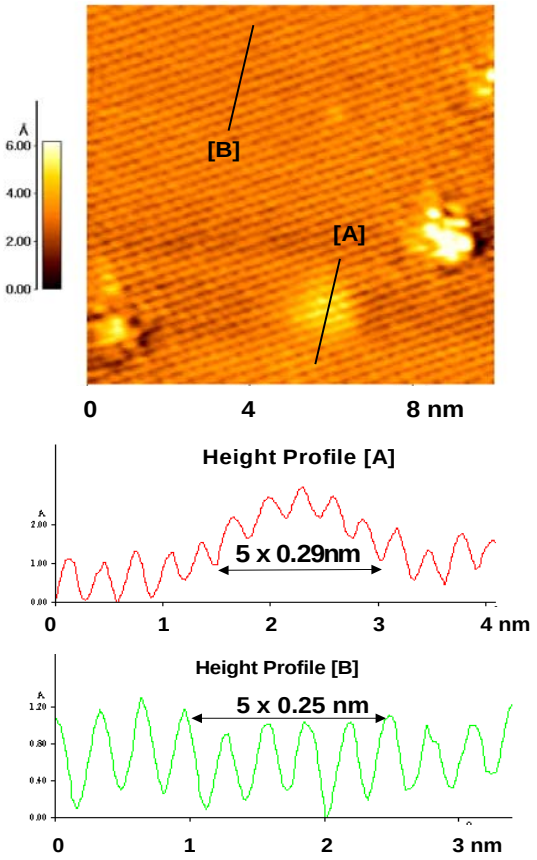

Fig. 6 STM image (10 nm x 10 nm) of isolated defects and the corresponding [A] and [B] profiles. On the [A] profile, the periodicity on the bump is 0.29 nm instead of 0.25 nm on the flat HOPG as plotted on the [B] profile.

atoms are observed, one out of three along the dense directions of the HOPG lattice. The corresponding 2D-FT exhibits two features: the largest hexagon stands for the HOPG lattice and the smallest one, 30° rotated, is due to the superstructure.

Such a $\sqrt{3}$x$\sqrt{3}$R30° periodic superstructure has already been reported on graphite surface around localized defects such as adsorbates, steps, outer crystal limit, adatoms, etc. [2–11,23–27]. It is the oscillatory response of an organized lattice to a localized perturbation of the electronic periodicity, that is to say the specific graphite shape of surface Friedel's [28] charge oscillations, with an oscillation period $\lambda_F = 3a$, λ_F being the Fermi wavelength and a the graphite lattice parameter a = 0.246 nm [29]. Regarding the origin of such defects, Hahn et al. pointed out that vacancies do not lead to $\sqrt{3}$x$\sqrt{3}$R30° periodic superstructure [6,9]. Moreover, DOS calculations do not predict superstructure around vacancies either [16,17]. Thus, the presence of this superstructure also supports the idea that the defects created by the plasma are not vacancies.

Although long time treated surfaces still remain globally conductive, STM observations were not as easy to perform on them as on short time treated samples, especially at small scale scans. On those surfaces several situations may be observed. Even if it is not possible by STM to clearly state whether the contrasted features are due to topography or to variations of the Fermi level CDOS, numerous highly perturbed areas are present, relatively broad and high, for which a real roughness (<1nm) can be deduced. As can be seen on Fig. 5d, other less protruding large features appear, on the top of which no fine features are evidenced i.e. neither the HOPG lattice nor defect structure. Moreover, the areas between those hillocks were difficult to image. Nevertheless, several STM images such as the one presented Fig. 5f were recorded on nearly flat parts of the surface but the graphitic regular lattice cannot be recognized at first glance. Spots are still visible on the two-dimensional

Fourier transform (2D-FT) and appear as two equal size hexagons 30° rotated. Removing one of the FT spot series, carbon atoms appear aligned in three directions, corresponding to the HOPG lattice orientations: the carbon atoms, even if still spaced about 0.25 nm apart along these linear segments, are no longer seen in their pristine ternary symmetry.

Thus after long treatment duration (30 minutes), the STM study shows that the whole outermost surface is modified, giving rise to great protruding hillocks or flat disordered zones. This conclusion is in very good agreement with the XPS analysis of the same sample, which also shows that all the surface carbon atoms contribute to the defect peak and are thus no longer in a graphitic state. UPS likewise, evidences that those atoms have lost their π orbitals.

We now examine whether, for the shorter treatment times, there is also quantitative correlation between the density of isolated defects, their associated superstructure and the C1s defect peak. In Table 1, the XPS C1s defect peak percentage is given, together with the "fraction of perturbed area", defined as the fraction of the total surface involved in defects, i.e. which gives a STM signal higher than the basal plane. For intermediate treatment times 5 and 15 min, the carbon population of the C1s defect peak corresponds to a measurable percentage, respectively 30 and 60 % of the outermost layer. In those cases, statistical analysis of the STM images requires thresholding which always leads to such large errors that the mean size values become meaningless. They are certainly smaller than 100%, but unfortunately no comparison may be made with the C1s defect peak population. However this fraction is clearly 100% for the totally perturbed surface (30 min treatment) and may be estimated at 3-6% for 1 min treatment, when taking into account the oscillating zones surrounding the isolated defects. After this last short treatment, the C1s spectrum is, as seen here above, already noticeably modified and the defect peak concerns 1-2% of the total observed population i.e. 2-4% of the external layers. This population is of the same order of magnitude as the STM perturbed area, which means that not only the 1 out of 10^3 C atoms involved in a defect, but also the carbon atoms surrounding it and submitted to the Friedel's electronic charge oscillations, participate in the shifted C1s peak.

In conclusion, we may say that the three techniques used, STM, XPS and UPS show the same evolution of the surface. The plasma treatment first creates isolated defects which become more numerous and finally invade the whole surface. The carbon atoms of this outermost surface, are not bound to heteroatoms but to their carbon neighbors in 3D bonds which are no longer of graphitic 2D type. It remains now to establish what the nature of these bonds is.

Carbon atoms are known to form many different types of chemical bonds which induce different structural conformations of the lattice in which they are included. Those

different C-C bonds are usually described by hybridization of sp^2 and sp^3 orbitals and many authors define them through a percentage of sp^3 character [30]. For instance in carbon nanotubes made up of rolled graphene planes, the sp^3 degree is estimated to be about 1%. Similarly in disordered carbon materials, this degree of hybridization may take different values [31,32]. In all the cases in which the sp^2 form is not pure, the carbon atoms do not form a completely flat plane and their XPS peak appears as +(0.5-1.0 eV) shifted relatively to pure graphite, the shift depending on the sp^3 percentage. Obviously, the diamond tetrahedral bond corresponds to the limiting 100% sp^3 value.

We believe the localized and stable defects produced on graphitic surface by low pressure plasma to be due to one or more carbon atoms slightly displaced out of their flat pristine sp^2 site and, in the sense defined above, which could be characterized by their percentage of sp^3 hybridization. Depending on the degree of the lattice disorder and on the magnitude of the displacements, this percentage may take different values and the entire defect population, defined by a distribution of sp^3 percentages, will give rise to a relatively broad XPS defect peak shifted from the pristine graphitic one. Such small displacements induce only small bulgings of the lattice, not high enough to be detected by the AFM technique. However they may induce a localized increase of the DOS and thus of the STM signal, which cannot be differentiated from the height atomic corrugation in a STM image. Around isolated defects, the carbon atoms submitted to Friedel's oscillations (oscillating DOS), may also be submitted to small oscillating displacements and their C1s electron binding energy may thus be slightly increased. Their photoelectrons will thus contribute to the XPS C1s defect peak.

The "geometrical" defects are not linked with any vacancy which would lead, in the case of extended defects, to real holes in the surface and to C-C bond breaking. The atomic displacements do not involve any dangling bonds. They are stable and they do not show any chemical reactivity.

Lastly, the assumption that our observed defects are only due to atomic displacements, an assumption corroborated by the results of the three techniques, is also in good agreement with the fact that such deformations have been created by very low energy ions of the argon plasma.

3 Conclusion

In this study we show that low energy Ar ions (E $\leq$ 20 eV) are able to create defects on an HOPG surface when they are produced in a plasma whereas a monokinetic Ar ion beam with energy lower than 40 eV has no effect. The synergy between the different plasma species such as electrons and metastable neutral atoms, is probably responsible for this effect .

The defects appearing as protrusions on STM images and leading to a broadening of the XPS C1s peak,

are stable both under vacuum and in air and, following our in situ XPS, UPS and STM results, we believe that they are not vacancies nor heteroatoms but small displacements of the carbon atoms from their pristine 2D graphitic sites. It could be expected that in similar studies involving low energy ions, the observed protuding features surrounded by Friedel's charge density oscillations also originate from atomic displacements rather than from vacancies or bonding to heteroatoms.

Aknowledgments. This work has been financially supported by the CNRS - Ultimatech program. We gratefully thank Pierre Lauginie and Jean-Paul Salvetat for highlighting discussions. The authors would like also to thank the referees for very helpful remarks and comments.

References

1. H. Brune, Surf. Sci. Rep. **31**, 121 (1998)
2. L. Porte, M. Phaner, C. H. Villeneuve, N. Moncoffre, J. Tousset, Nucl. Instrum. Meth. B **44**, 116 (1989)
3. J. R. Hahn and H. Kang, Surf. Sci. **357 - 358**, 165 (1998)
4. R. Coratger, A. Claverie, A. Chahboun, V. Landry, F. Ajustro, J. Beauvillain, Surf. Sci.**262**, 208 (1992)
5. D. Marton, H. Bu, S.S. Todorov, K. J. Boyd, A. H. Al-Bayati, J. W. Rabalais, Surf. Sci. Lett. **326**, L489 (1995)
6. J. R. Hahn, H. Kang, S. Song, I. C. Jeon, Phys. Rev. B **53**, R1725 (1996)
7. K. Mochiji, S. Yamamoto, H. Shimizu, S. Ohtani, T. Segushi, N. Kobayashi, J. Appl. Phys. **82**, 6037 (1997)
8. H. Ogisho, W. Mizutani, S. Nakano, H. Tokumoto, K. Yamanaka, Appl. Phys. A **66**, S1155 (1998)
9. J. R. Hahn, H. Kang, Phys. Rev B. **60**, 6007 (1999)
10. P. Ruffieux, O. Gröning, P. Schwaller, L. Schlapbach, P. Gröning, Phys. Rev Lett. **84**, 4910 (2000)
11. E. Bourelle, H. Konno and M. Inagaki, Carbon **37**, 2041 (1999)
12. A. L. Thomann, C. Charles, P. Brault, C. Laure, R. Boswell, Plasma Sources Sci. Technol. **7**, 245 (1998)
13. D. Marton, K. J. Boyd, T. Lytle, J. W. Rabalais, Phys. Rev B **48**, 6757 (1993)
14. K. J. Boyd, D. Marton, J. W. Rabalais, S. Uhlmann, Th. Frauenheim , J. Vac. Sci. Technol. A **16**, 444 (1998)
15. B. Rousseau, H. Estrade-Szwarckopf, Solid State Comm. **85**, 795 (1993)
16. K. H. Lee, H. M. Lee, H. M. Eun, W. R. Lee, S. Kim, And D. Kim, Surf. Sci.**321**, 267 (1994)
17. A.V.Krasheninnikov, V.F. Elesin, Surf. Sci. **454-456**, 519-524 (2000)
18. Y. Yamamura, H. Tawara, NIFS-DATA Series **23**, 1 (1995)
19. C. Paturaud, G. Farges, M. C. Sainte Catherine, J. Machet, Surf. Coat. Technol. **98**, 1257 (1998)
20. W. D. Davis, T. A. Vanderslice, Phys. Rev. **131**, 219 (1963)
21. A. Manenshijn, G. C. A. M. Janssen, E. van der Drift, S. Radelaar, J. Appl. Phys. **69**, 1253 (1991)
22. J. Coburn, H. F. Winters, J. Appl. Phys. **50**, 3189 (1979); J. Vac. Sci. Technol **16** 391 (1980)

23. A. Humbert, M. Dayez, S. Sangay, C. Chapon, C. CR. Henry, J. Vac Sci. Technol. A **8**, 311 (1990)

24. J. Xhie, , K. Sattler, U. Müller, N. Venkateswaran, G. Raina, Phys. Rev. B **43**, 8917 (1991)

25. L. Porte, M. Phaner, C. Noupa, B. Tardy, J. C. Bertolini, Ultramicroscopy **42-44**, 1355 (1992)

26. F. J. C. Santos Aires, P. Sautet, G. Fuchs, J.-L. Rousset, P. Mélinon, Microsc. Microanal. Microstruct. **4**, 441 (1993)

27. E. Lacaze, Thesis, Université Paris VII (1991)

28. J. Friedel, Phil. Mag. **43**, 153 (1952)

29. A. Rubio, D. Sanchez-Portal, E. Artacho, and P. Ordejon, Phys. Rev. Lett. **82** 3520 (1999)

30. P. Delhaès, in *Le carbone dans tous ses états* , Eds. P. Bernier and S. Lefrant (Gordon and Breach Science, Amsterdam, 1997) p. 41; T. Ebbesen, *ibid* p.187 . See also the english translation : *Carbon Molecules and Materials*, Ed. R. Setton, P. Bernier, S. Lefrant (Taylor & Francis, London 2002) p. 51 and p.179, respectively).

31. J. Diaz, G. Paolicelli, S. Ferrer, F. Comin, Phys. Rev. B **54**, 8064 (1996)

32. S. Rey, F. Antoni, B. Prevot, E. Fogarassy, J. C. Arnault, J. Hommet, F. Lenormand, P. Boher, Appl. Phys. A**71**, 433 (2000)